

Behavior and Testing of Anchors in Simulated Seismic Cracks

by Matthew S. Hoehler and Rolf Eligehausen

This paper deals with the behavior and testing of cast-in-place and post-installed anchors in cracked concrete where the cracks are repeatedly opened and closed. This condition can be decisive for determining the suitability of an anchor for earthquake applications. First, the results of investigations to establish representative crack cycling conditions for anchors during an earthquake are summarized. Second, new experimental tests with headed studs and four types of post-installed anchors under simulated seismic crack cycling conditions are presented and discussed. The discussion focuses on the behavior of different anchor failure modes, the influence of the anchor head bearing pressure, and the magnitude of the compression load applied to the concrete member to affect crack closure.

Keywords: anchor; crack cycling; cracked concrete; earthquake; testing.

INTRODUCTION

Cast-in-place and post-installed mechanical and adhesive anchors are frequently used to secure nonstructural elements and to connect new structural elements to existing structures in earthquake retrofit designs. Though it is often presumed that anchor response to the cracking that may occur in a reinforced concrete structure during an earthquake will be decisive in determining the anchor's suitability for seismic applications,¹ experimental evidence is limited to cracks that never fully close.²⁻⁶ Moreover, the existing crack cycling test in ACI 355.2-04,⁷ which is required as part of the prequalification of post-installed anchors for seismic use, applies testing methods and assessment criteria developed to represent service crack cycling conditions, for example, crack width variations due to changes in live loads and thermal loads over the life of a structure rather than seismic conditions.

RESEARCH SIGNIFICANCE

This paper presents the first published data on the performance of anchors during crack cycling where cracks are pressed fully closed by an external force on the concrete member. The results provide new understanding of anchor behavior under earthquake conditions and background for the development of improved prequalification methods for anchors used in seismic regions.

BACKGROUND FOR TESTING PARAMETERS

Earthquakes affect anchors in two significant ways. First, they cause cracking and crack cycling in the primary structure that serves as the anchorage material. Second, the motion of the primary structure generates actions on secondary structures, which, in turn, generate dynamic tension and shear forces on anchors (Fig. 1). In this paper, the focus is on the crack cycling behavior.

As the primary structure responds to earthquake ground motion, it experiences displacements and consequently

deformation of its members. These deformations lead to the formation and opening of cracks. Regions of inelastic deformation can often be distinguished (Fig. 2).

When the direction of displacement of the primary structure changes, for example, from right to left in Fig. 2, moment reversal will occur in some members and cracks that had been opened during a previous displacement cycle will be pressed closed. Therefore, to assess the performance of anchors in concrete during an earthquake, it is necessary to understand their behavior in cycled cracks. The expected crack opening-and-closing widths, as well as the number of crack cycles, are critical parameters.

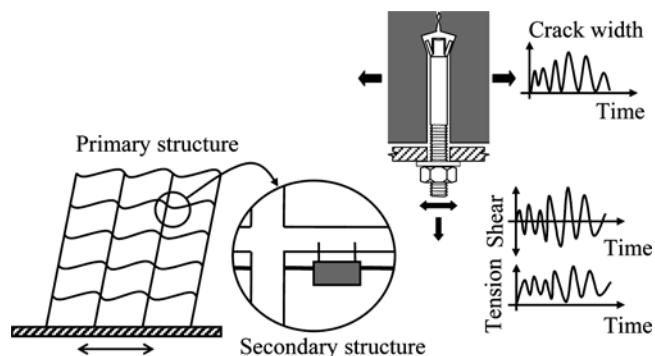


Fig. 1—Actions acting on nonstructural anchorage under earthquake loading.

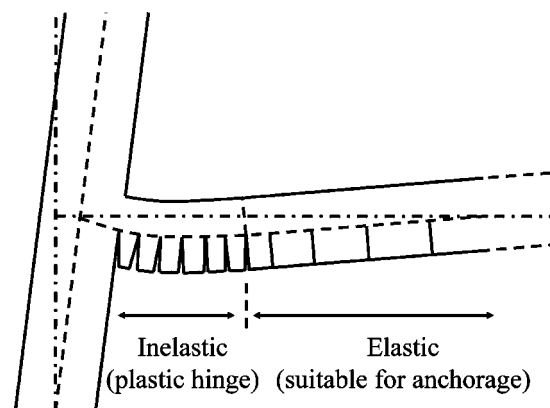


Fig. 2—Idealization of cracking in beam caused by transverse motion of building.

ACI Structural Journal, V. 105, No. 3, May-June 2008.

MS No. S-2007-004.R1 received February 8, 2007, and reviewed under Institute publication policies. Copyright © 2008, American Concrete Institute. All rights reserved, including the making of copies unless permission is obtained from the copyright proprietors. Pertinent discussion including author's closure, if any, will be published in the March-April 2009 *ACI Structural Journal* if the discussion is received by November 1, 2008.

ACI member **Matthew S. Hoehler** is Director of Research for Hilti North America, Encinitas, CA. He received his BS in civil engineering from Princeton University, Princeton, NJ; his MSc in civil engineering from the University of California-Berkeley, Berkeley, CA; and his PhD from the Institute of Construction Materials, Universität Stuttgart, Stuttgart, Germany.

Rolf Eligehausen, FACI, is a Professor and Head of the Department of Fastening Technology at the Institute of Construction Materials, Universität Stuttgart. He is a member of ACI Committees 349, Concrete Nuclear Structures; 355, Anchorage to Concrete; and 408, Bond and Development of Reinforcement. His research interests include research and testing of anchor technology.

Crack width and cycling

The seismic design guidelines for anchors in Appendix D of ACI 318-05⁸ are only applicable to anchors located outside of plastic hinge zones (Section D.3.3.1). This is reasonable because spalling of the concrete cover and large crack widths inside of a plastic hinge will reduce the anchor capacity significantly and make anchoring impractical.

Outside of the plastic hinge, the maximum crack opening width that can occur is that when the steel reinforcement in the anchorage component just reaches yield strain. This is the maximum crack opening width for which anchors need to be tested when they are used to resist earthquake loads according to ACI 318-05.⁸

Extensive numerical studies of crack width in reinforced concrete bending members designed according to Eurocode 2⁹ indicate that the maximum crack width that can be expected to occur at steel yield in unfavorably designed flexural members is approximately 0.8 mm (0.03 in.).¹⁰ This value was determined for frame members subjected primarily to axial and bending deformation and is not valid for shear cracking.

The degree to which a previously opened crack will close during a moment reversal depends on several factors including:

- The width to which the crack was previously opened;
- The amount of reinforcement steel that crosses the crack;
- The level of the acting compression force; and
- The possible presence of an anchor in the crack that produces splitting forces that hold the crack open.

For the purpose of anchor testing, it must be assumed that the type of member in which the anchor will be installed, for example, in a beam, column, slab, or wall, is not restricted. Therefore, anchor performance under the conditions present in a member with an axial compression load and symmetric moment reversals, for example, a column or wall, should be verified. In such members, it is likely that full crack closure will occur. Current testing procedures⁷ do not require full crack closure during crack cycling, but rather, they are designed to permit the crack width at zero member tension load to be governed by the steel reinforcement ratio, bond degradation, and anchor response throughout the course of the test.

Number of crack cycles

The number of times a crack in a reinforced concrete member will open and close during an earthquake depends on the number of deformation cycles to which the member is subjected. Because earthquake shaking is irregular, some ground motion pulses will result in larger inelastic deformations of the member than others. The magnitude of the inelastic deformation inside of the plastic hinge zone is not relevant for the crack opening width outside of this zone, however, because the steel strain at the edge of the plastic hinge is, by definition, at yield. Crack closing widths depend on the level

of the resultant compressive force at the crack location. If it is assumed that only the largest amplitude deformation cycles during an earthquake lead to complete crack closure, then it would be useful to define an equivalent number of uniform-amplitude inelastic cycles at the maximum amplitude that will cause the same amount of damage to the structure as the total number of nonuniform deformations. This has been done by several investigators for various structure types and earthquake ground motions.¹¹⁻¹⁴

Based on the results in these studies, 10 ($n_{eq} = 10$) symmetric, uniform-amplitude, inelastic cycles at maximum amplitude are taken to be representative of the number of crack opening-and-closing cycles during an earthquake for anchor testing purposes.¹⁰

EXPERIMENTAL PROGRAM

A test setup was developed to simulate the seismic crack cycling conditions described previously. The effect of simultaneous crack and load cycling was neglected and a constant axial seismic design load on the anchor was assumed. This simplification allowed the behavior arising from crack cycling to be isolated.

Investigated anchors

Figure 3 schematically illustrates the investigated anchor types. Detailed descriptions of the various anchor types and their load transfer mechanisms can be found in Eligehausen et al.¹⁵ The relevant anchor parameters are summarized in Table 1. Anchors with similar outside diameters but distinctly different failure modes were selected. The anchors were installed according to the manufacturers'

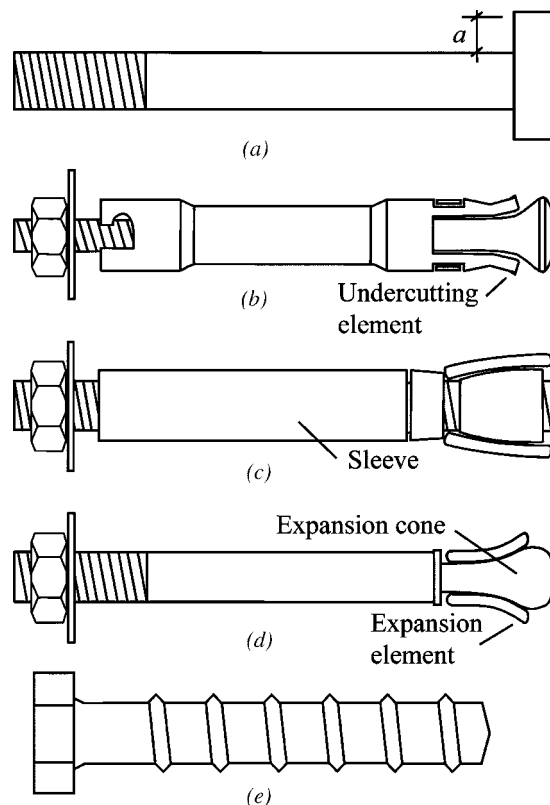


Fig. 3—Investigated anchor types: (a) headed stud; (b) undercut anchor; (c) expansion anchor (sleeve-type); (d) expansion anchor (bolt-type); and (e) screw anchor.

recommendations, except where the effective embedment depth h_{ef} was modified to achieve a desired failure mode (refer to Table 1). The preloading torque on the expansion and undercut anchors was reduced to 50% of the recommended installation value immediately prior to testing to simulate relaxation over time as can be expected under field conditions. The screw anchors were tested with the full recommended installation torque. No installation torque was required for the headed studs. All of the tested anchors except the screw anchors had a European Technical Approval for use in cracked concrete.

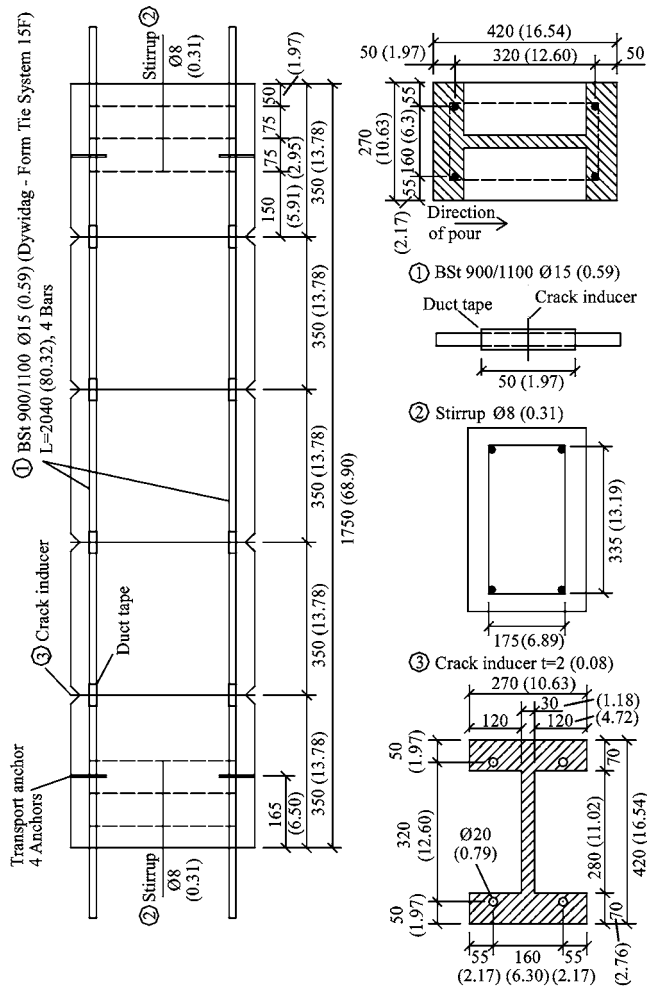


Fig. 4—Anchorage component for seismic crack cycling tests. (Note: 1 mm = 0.0394 in.)

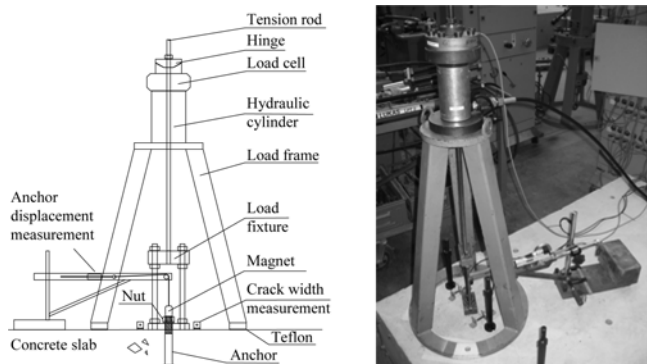


Fig. 5—Loading setup for reference tension tests in static line cracks.

Anchorage components

Monotonic tension tests in static cracks (reference tests) were conducted in reinforced concrete slabs (1635 x 1550 x 260 mm [64 x 61 x 10 in.]) made of normal-strength concrete. The slabs were designed to allow for the formation and control of static line cracks using steel splitting wedges driven into sleeves placed in preformed holes in the slab. Details on this method of crack formation are provided by Eligehausen et al.¹⁶

The simulated seismic crack cycling tests were performed in reinforced concrete members (1750 x 420 x 270 mm [69 x 17 x 11 in.]) made of normal-strength concrete (Fig. 4). Special, high-strength steel reinforcement bars with a rib pattern that allowed for special nuts to be screwed onto the bars were used for the longitudinal reinforcement. Four I-shaped, thin (2 mm [0.08 in.]) metal plates (crack inducers) were placed along the member at the average calculated crack spacing ($s_{cr} = 350$ mm [14 in.]) to aid crack formation. Duct tape was used to destroy the bond between the concrete and the reinforcement bars in a small region (± 25 mm [1 in.]) to either side of the crack inducer, which made it easier to generate large crack opening widths.

All concrete specimens were fabricated in accordance with DIN 1045¹⁷ and DIN 1048.¹⁸ The average concrete cube (150 mm [6 in.]) compressive strength for the members at the time of testing varied from $f_{cc,150} = 25.7$ N/mm² (3.7 ksi) to $f_{cc,150} = 31.5$ N/mm² (4.6 ksi).

Reference tension tests

Reference tests in static line cracks were performed using the test setup in Fig. 5. These tests were performed on single anchors with anchor spacing and edge distances reasonably selected for the desired failure modes to avoid influence from adjacent anchors or edges of the test specimen. The load cylinder support frame was located at a clear distance of at least $1.5 \times h_{ef}$ from the anchor (unconfined test). The anchor was installed in a closed hairline crack ($w \approx 0.05$ mm [0.002 in.]), which was then opened by $\Delta w = 0.8$ mm (0.03 in.) before loading of the anchor. Tension load was applied to the anchor using a hydraulic cylinder with a load capacity of 100 kN (22.5 kip) by slowly increasing the oil volume in the cylinder (pseudo displacement-controlled). Ultimate load was reached in approximately 1 to 3 minutes. Crack widths were monitored, but not controlled, during loading.

Table 1—Investigated anchor parameters

Anchor type	Size, mm (in.)	Drill hole diameter d_0 , mm (in.)	Effective embedment h_{ef} , mm (in.)	Failure mode*
Headed stud† (Grade St37)	$d = 19$ (0.75)	—	100 (3.94)	Concrete cone
Undercut anchor	M10 (0.39)	20 (0.79)	80‡ (3.15)	Concrete cone
Expansion anchor (sleeve-type)	M12 (0.47)	18 (0.71)	80 (3.15)	Concrete cone
Expansion anchor (bolt-type)	M16 (0.63)	16 (0.63)	95§ (3.74)	Pull-through
Screw anchor	$d = 120$ (0.79)	18 (0.71)	76 (2.99)	Pullout/concrete cone

*Failure mode dictated by chosen installation parameters.

†Under cut length $a = 3.75$ mm (0.15 in.) (refer to Fig. 3).

‡Actual h_{ef} = recommended h_{ef} - 20 mm (0.79 in.).

§Actual h_{ef} = recommended h_{ef} + 10 mm (0.39 in.).

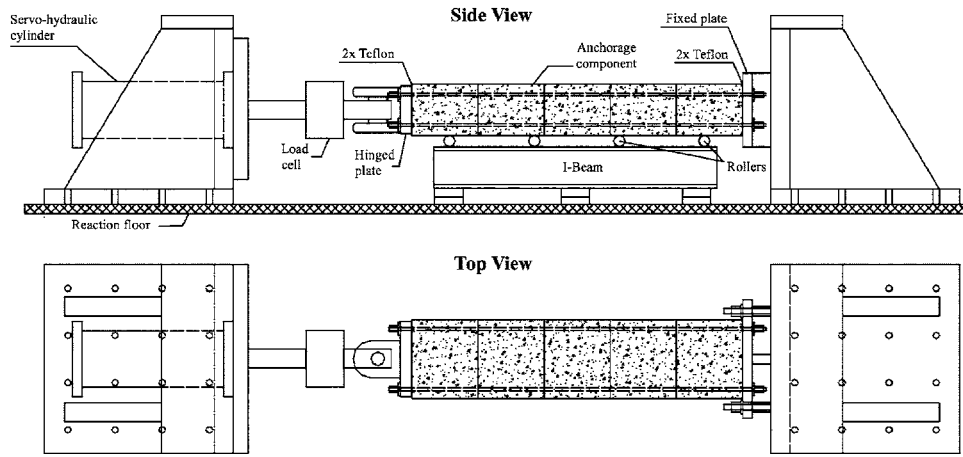


Fig. 6—Loading setup for seismic crack member.

Table 2—Critical events during loading time-histories

Time	Critical event
t_1	Crack opening to w_1
t_2	Anchor loading to N_w
t_3	First crack closing
t_4	Start of crack cycling
t_5	End of crack cycling
t_r	Measurement of residuals
t_7	Crack reopening
t_u	Ultimate strength during pullout

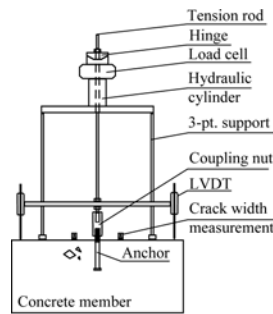


Fig. 7—Anchor loading setup for seismic crack cycling tests.

Seismic crack cycling tests

For the seismic crack cycling tests, four line cracks were generated in the special anchorage components (Fig. 4) using the setup in Fig. 6. The cracks were opened via tensile force applied to the longitudinal reinforcement bars. The cracks were closed by applying compressive force distributed over the ends of the component.

Anchors were installed in all four cracks in the member and loaded simultaneously with a constant tension load N_w during crack cycling. If not noted otherwise, N_w was equal to 40% of the mean anchor failure load ($N_{u,m}$) obtained from a static reference test ($N_w = 0.4N_{u,m}$). The anchor loading setup is shown in Fig. 7. All tests were performed with anchor spacing and edge distances reasonably selected for the desired failure modes to avoid influence from adjacent anchors or edges of the test specimen. Furthermore, the load setup allowed for development of a full concrete cone (unconfined test).

After crack cycling, pullout tests were performed sequentially along the member using a setup similar to that in Fig. 5 to determine the residual strengths of the tested anchors.

Loading time-histories for the anchors and the anchorage component are shown schematically in Fig. 8. Table 2 lists critical events in the time-histories. The headed studs were installed prior to Phase I in Fig. 8, that is, during casting of the specimen, but were not axially loaded until the time indicated in the figure. The load applied to the anchors N_w , the anchorage component load levels $F_{m,1}$, $F_{m,2}$, and number of crack cycles n varied. The value of $F_{m,1}$ designates the member load required to attain the prescribed crack opening width w_1 . The value of $F_{m,2}$ is the member load required to attain the prescribed crack closing width w_2 or the prescribed

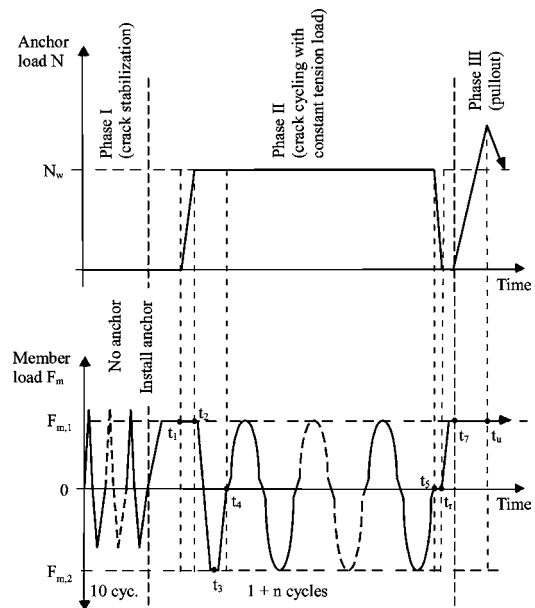


Fig. 8—Schematic loading time-histories for anchor and anchorage component.

compression load level F_2 . The variable Δw is used to designate the measured crack opening width beyond the initial hairline crack width.

EXPERIMENTAL RESULTS AND DISCUSSION

Anchor behavior in cycled cracks

The load-bearing and displacement mechanisms of anchors in opening and closing cracks under service conditions were

described by Lotze and Faoro.⁶ Their work is presented herein with a slight modification for the case of seismic conditions.

Figure 9 schematically illustrates the behavior of an undercut anchor in an opening and closing crack. Before the first crack opening, the anchor bears directly on the surface of the undercut in the concrete (Fig. 9(a)). During the first crack opening (Fig. 9(b)), the anchor must displace in the direction of the applied load by $\Delta\delta_{11}$ to fulfill equilibrium and compatibility conditions. If the crack is then partially or completely closed, the undercutting elements of the anchor will be deformed and pressed into the concrete (Fig. 9(c)). For some anchor geometries, if sufficiently large compressive stress is applied, displacement $\Delta\delta_{12}$ opposite to the direction of the applied load will occur. During the next crack opening, the displacement $\Delta\delta_{12}$ and the elastic portion of the deformation in the expansion elements and the concrete is recovered and the anchor will displace again in the direction

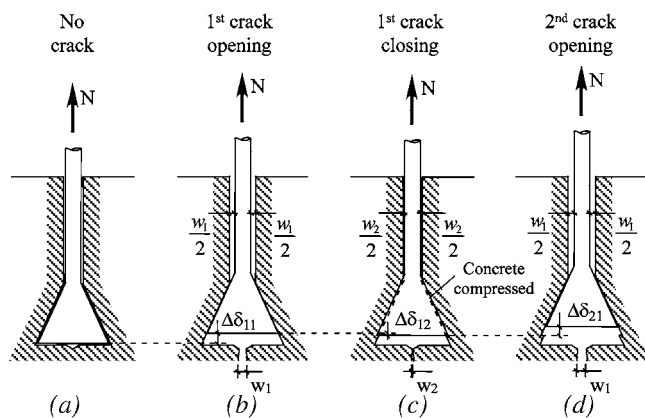


Fig. 9—Load-bearing and displacement mechanisms for anchors in opening and closing cracks (after Lotze and Faoro⁶).

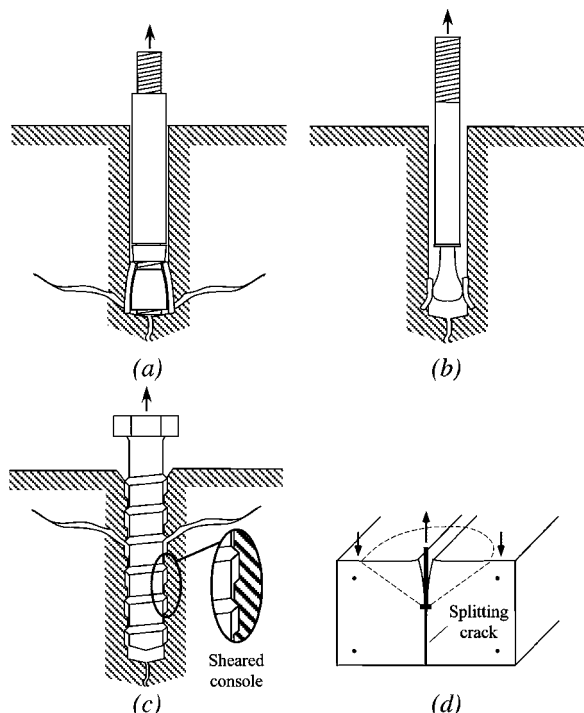


Fig. 10—Failure modes: (a) concrete cone breakout; (b) pull-through; (c) pullout/concrete cone; and (d) splitting.

of the applied load ($\Delta\delta_{21}$) to reestablish equilibrium (Fig. 9(d)). This mechanism is valid for subsequent crack cycles. The main effect of applying compression stress to the concrete is the local damage of the anchorage material and the consequently large magnitudes of displacements $\Delta\delta_{11}$ and $\Delta\delta_{21}$.

The load-bearing and displacement mechanisms described previously apply to many anchor types that transfer tension load from the anchor to the concrete primarily by mechanical interlock, for example, headed studs, undercut anchors, and screw anchors. For anchors that transfer tension load primarily by friction (for example, expansion anchors), the concept of displacement advance and arrest to satisfy force equilibrium and compatibility during crack cycling as described previously applies. The displacement mechanisms, however, will differ slightly depending on the location of the friction slip. The displacements $\Delta\delta$ can occur either at the interface between the expansion elements and the drilled hole or at the interface between the anchor expansion cone and the expansion elements (refer to Fig. 3).

Failure modes

Depending on the anchor type and installation parameters, crack cycling under seismic conditions can result in concrete cone breakout (Fig. 10(a)), pull-through (the expansion elements remain in the drilled hole) (Fig. 10(b)), pullout (including the anchor expansion or undercutting elements) (Fig. 10(c)), or splitting of the anchorage component during crack cycling (Fig. 10(d)). If no failure occurs during crack cycling, all applicable failure modes (refer to ACI 318-05⁸) apply during subsequent loading.

The investigated headed studs, undercut anchors, and sleeve-type expansion anchors failed by concrete cone breakout in pullout tests performed in an open crack ($\Delta w = 0.8$ mm [0.03 in.]) subsequent to 10 large crack opening-and-closing cycles ($w_1 = 0.8$ mm [0.03 in.]; $w_2 = 0.0$ mm) with a constant anchor tension load $N_w = 0.4N_{u,m}$. The bolt-type expansion anchors failed by pull-through, and the screw anchors failed by pullout subsequent to the previously described crack cycling.

Concrete cone breakout

The current investigation shows that the load-displacement behavior of anchors failing by concrete cone breakout in reference tests and in representative seismic crack cycling tests is essentially the same as described by Furche¹⁹ for headed studs under service crack cycling conditions ($N_w = 0.3N_{u,m}$, $w_1 = 0.3$ mm [0.01 in.], $w_2 = 0.1$ mm [0.004 in.], and $n = 1000$); however, the displacement increase during seismic crack cycling is much larger.

Furche¹⁹ shows that if the axial anchor displacement during 1000 crack cycles (δ_{1000}) plus the additional displacement up to ultimate load obtained in a subsequent pullout test ($\delta_{u,add}$) is smaller than the displacement at ultimate load in a comparable monotonic test ($\delta_{u,m}$), the ultimate load is not affected by the crack cycling. If the combined anchor displacement $\delta = \delta_{1000} + \delta_{u,add}$ exceeds $\delta_{u,m}$, the ultimate load decreases as a function of the lost anchor embedment depth according to $C(h_{ef} - \delta)^{1.5}$, where C is an empirical constant (Fig. 11).

In crack cycling tests representative of seismic conditions, the large crack cycling widths, high anchor loads, and the application of compressive load to the anchorage component to achieve crack closure can result in anchor displacements that exceed those at ultimate load in monotonic reference tests in fewer than 10 crack cycles. This is shown in Fig. 12

Table 3—Displacement conditions during crack cycling for concrete cone breakout

Condition	Description	Residual strength
(1) $\delta_{10} < \delta_{u,m}$	Displacement during crack cycling is less than that at ultimate load in monotonic reference tests	$N_{u,c} \geq N_{u,m}$
(2) $\delta_{u,m} \leq \delta_{10} < \delta_{f,c}$	Displacement during crack cycling equals or exceeds that at ultimate load in monotonic reference tests but does not reduce effective anchorage depth enough to result in concrete cone breakout at applied constant tension load	$N_{u,c} < N_{u,m}$
(3) $\delta_{10} = \delta_{f,c}$	Displacement during crack cycling reduces effective anchorage depth enough to result in concrete cone breakout at applied constant tension load	Not applicable

for the three tested anchor types that failed by concrete cone breakout. Because anchor displacement during crack cycling is a function of the number of crack cycles (which was limited in the tests to 10), in general, the amount of displacement beyond $\delta_{u,m}$ was small and did not reduce the effective anchorage depth enough to result in a significant decrease of the residual strength. In fact, the residual strength of the headed studs actually increased relative to the ultimate strength in the reference tests (Fig. 12(a)). This is believed to be due in part to compaction of the concrete around the head of the anchor during crack cycling. For the investigated undercut anchors, the residual capacity was approximately equal to the capacity measured in reference tests (Fig. 12(b)). At some displacement, however, the reduction of the effective anchorage depth due to crack cycling will reduce the residual capacity of the anchor. This behavior was observed for one of the tested sleeve-type torque-controlled expansion anchors (Fig. 12(c)).

The important conclusion is that as long as the effective anchorage depth is not reduced too significantly during crack cycling, the residual strength will be approximately the same as in monotonic reference tests for the case of concrete cone breakout.

The slight fluctuation of the anchor load during crack cycling in Fig. 12 is a physical phenomenon resulting from closure of the crack. Because the oil volume in the hydraulic cylinders was used to regulate the anchor load, the anchor load increased as the anchor was pressed back into its hole during crack closure (refer to Fig. 9).

Three cases can be distinguished based on the amount of displacement that occurs during crack cycling. These are summarized in Table 3 and illustrated in Fig. 13. The anchor displacement that occurs during 10 crack cycles is designated as δ_{10} . The displacement at which the curve $C \times (h_{ef} - \delta)^{1.5}$ is intersected is designated as $\delta_{f,c}$. Additionally, in the case of thin or narrow members, splitting of the anchorage component may occur as a result of wedging forces generated by the anchors during crack cycling.

Pull-through failure of mechanical anchors

The behavior of a bolt-type expansion anchor failing by pull-through in reference tests and in tests subsequent to repeated large crack opening and closing cycles is shown in Fig. 14. In the case of pull-through failure where the expansion elements do not slip in the drilled hole, the load-displacement curve is bounded by the descending branch of the monotonic load-displacement curve.

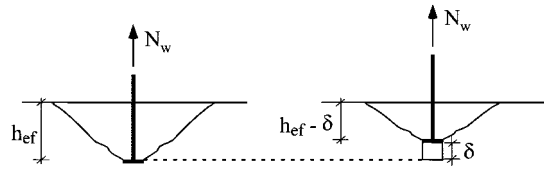


Fig. 11—Reduction of embedment depth.

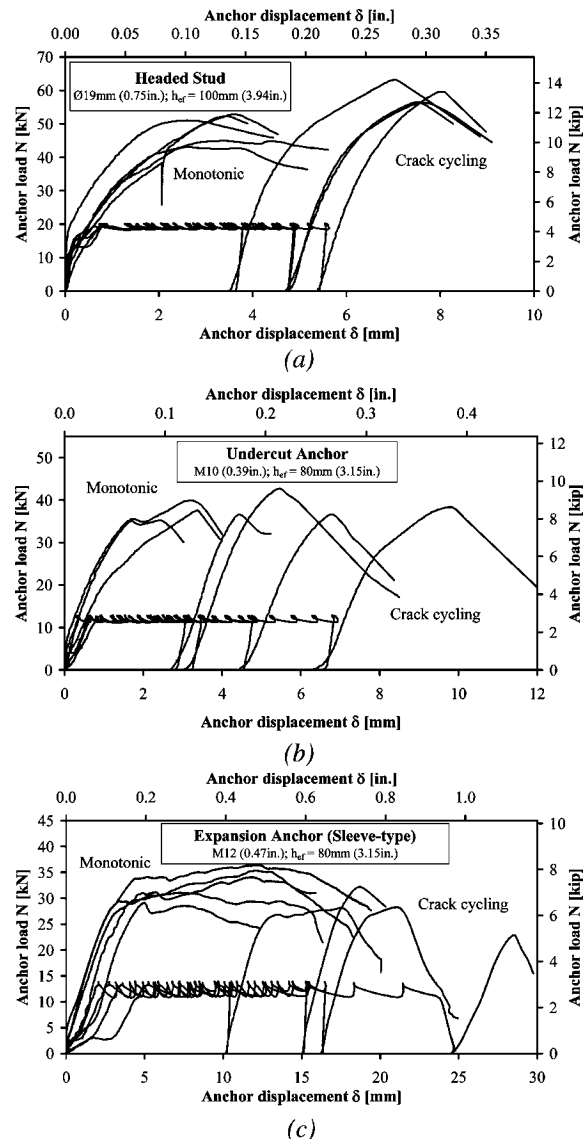


Fig. 12—Load-displacement curves for monotonic ($w = 0.8 \text{ mm}$ [0.03 in.]) and crack cycling ($w_1 = 0.8 \text{ mm}$ [0.03 in.]; $w_2 = 0.0 \text{ mm}$; $n = 10$; $N_w = 0.4 \times N_{u,m}$) tests: (a) headed studs; (b) undercut anchors; and (c) expansion anchors (sleeve-type).

Taking into account the results of tests described by Rehm and Lehmann² and the tests performed in this study, three cases can be distinguished based on the amount of displacement that occurs during crack cycling. These are summarized in Table 4 and illustrated in Fig. 15. The displacement at which the descending branch of the monotonic curve is intersected is designated as $\delta_{f,pr}$.

Pullout failure of screw anchors

The investigated screw anchor ($d = 20 \text{ mm}$ [0.79 in.]) failed in mixed pullout and concrete cone breakout in monotonic

tests in cracked concrete ($\Delta w = 0.8 \text{ mm}$ [0.03 in.]), that is, the lower portion of the screw pulled out and a concrete cone formed near the surface of the concrete. In pullout tests performed after the crack cycling, pure pullout failure occurred. Figure 16 compares the monotonic and crack cycling load-displacement behavior. Had the anchors failed in pure pullout failure in both the monotonic and crack cycling tests, it is expected that the load-displacement behavior would be similar to that described for pull-through failure, that is, the load-displacement curve for the crack cycling test is bounded by the descending branch of the monotonic load-displacement curve.

The large displacements during crack cycling in Fig. 16 were possible due to the large thread spacing ($\sim 15 \text{ mm}$

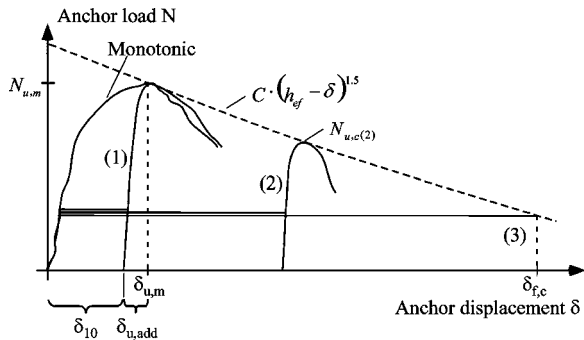


Fig. 13—Schematic load-displacement curves for crack cycling tests in case of concrete cone breakout.

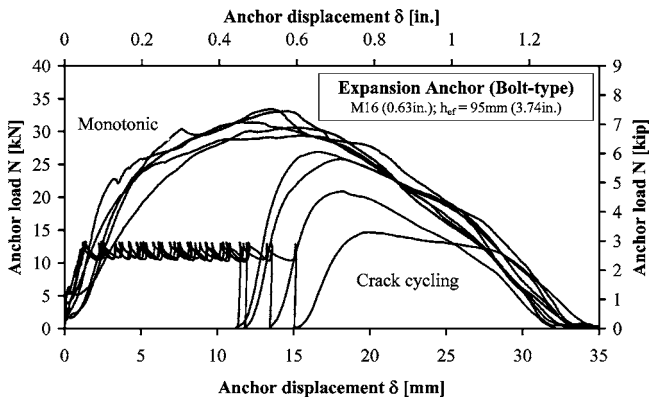


Fig. 14—Load-displacement curves for monotonic ($w = 0.8 \text{ mm}$ [0.03 in.]) and crack cycling ($w_1 = 0.8 \text{ mm}$ [0.03 in.]; $w_2 = 0.0 \text{ mm}$; $n = 10$; $N_w = 0.4 \times N_{u,m}$) tests for pull-through ($\delta_{10} \approx \delta_{u,m}$).

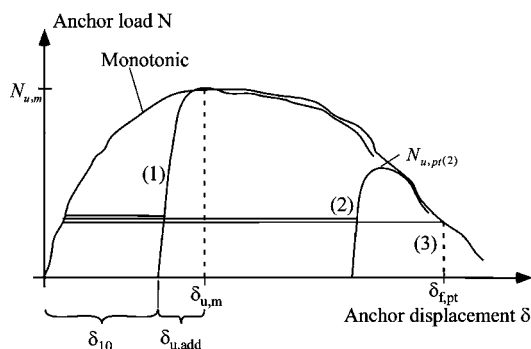


Fig. 15—Schematic load-displacement curves for crack cycling tests in case of pull-through.

[0.59 in.] of the investigated screw anchors. For screw anchors with smaller thread spacing, significantly smaller displacement capacity during crack cycling is expected.

Anchor displacement

The displacement behavior of the investigated anchors during crack cycling representative of seismic conditions ($w_1 = 0.8 \text{ mm}$ [0.03 in.]; $w_2 = 0.0 \text{ mm}$; and $n = 10$) is shown in Fig. 17. The curves show the total displacement of the anchor recorded at each crack-opening cycle. Each curve represents the average of three or more test replicates. In all cases, failure occurred during the subsequent pullout test.

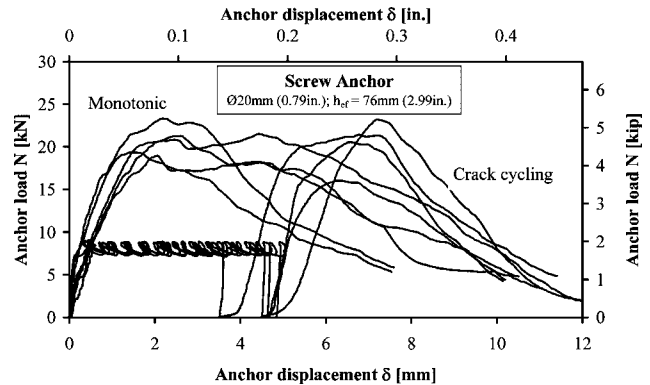


Fig. 16—Load-displacement curves for monotonic ($w = 0.8 \text{ mm}$ [0.03 in.]) and crack cycling ($w_1 = 0.8 \text{ mm}$ [0.03 in.]; $w_2 = 0.0 \text{ mm}$; $n = 10$; $N_w = 0.4 \times N_{u,m}$) tests for pullout of screw anchors.

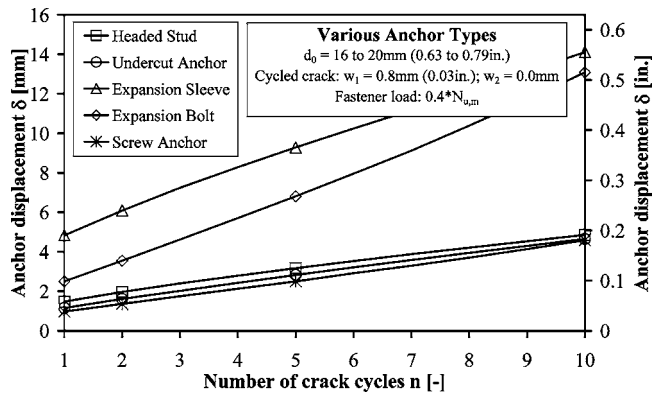


Fig. 17—Anchor displacement as function of number of crack cycles for investigated anchors.

Table 4—Displacement conditions during crack cycling for pull-through failure

Condition	Description	Residual strength
(1) $\delta_{10} < \delta_{u,m}$	Displacement during crack cycling is less than that at ultimate load in monotonic reference tests	$N_{u,pt} \geq N_{u,m}$
(2) $\delta_{u,m} \leq \delta_{10} < \delta_{f,pt}$	Displacement during crack cycling equals or exceeds that at ultimate load in monotonic reference tests but is less than displacement at intersection of applied constant anchor load with monotonic envelope	$N_{u,pt} < N_{u,m}$
(3) $\delta_{10} = \delta_{f,pt}$	Displacement during crack cycling reaches displacement at intersection of applied constant anchor load with monotonic envelope	Not applicable

Figure 17 shows that for all tested anchors except the bolt-type expansion anchor, the displacement increase as a function of the number of crack cycles was degressive or nearly linear. Note that the displacements are plotted as a linear function of the number of crack cycles. This differs from previous studies with service crack cycling conditions where displacements are plotted as a function of the logarithm of the number of crack cycles.

Degrressive or linearly increasing anchor displacements with increasing crack cycles (linear-linear scale) is one indicator of acceptable anchor performance (Fig. 18). This is substantiated by the results in the following section. When analyzing the resistance of anchor groups, however, acceptable anchor displacements during crack cycling must consider the effect of the magnitude of displacement on load distribution to the anchors in the group, that is, not just the rate of displacement increase. Further research is needed to quantify this limiting value.

Influence of anchor bearing pressure

Figure 19 shows anchor displacements as a function of the number of crack cycles for headed studs ($h_{ef} = 100$ mm [3.94 in.], $d = 19$ mm [0.75 in.], and $d_h = 26.5$ mm [1.04 in.]) subjected to large crack opening and closing cycles ($w_1 = 0.8$ mm [0.03 in.], $w_2 = 0.0$ mm, and $n = 10$), where the constant tension loads on the anchors were chosen to produce head bearing pressures ($p = N_w/A_h$) of $4.0 \times f_{cc,150}$, $2.5 \times f_{cc,150}$, or $1.0 \times f_{cc,150}$. The bearing pressure $2.5 \times f_{cc,150}$ roughly corresponds to the current allowable bearing pressure for headed studs of $8 \times f_c$ in cracked concrete⁸ factored by 40% to represent the design load level for seismic applications ($0.4 \times [8 \times f_c] = 3.2 \times f_c \approx 2.5 \times f_{cc,150}$).

The increase of anchor displacement during crack cycling depends significantly on the pressure under the head. The test results indicate that the existing limit for allowable bearing pressure used for nonseismic applications ($8 \times f_c$) is also suitable for crack cycling representative of seismic situations. Higher head bearing pressure ($4.0 \times f_{cc,150}$) led to progressively increasing displacements and a significant drop in the residual strength of the anchor (Fig. 20). The ultimate loads in Fig. 20 have been normalized to a concrete strength of 30 N/mm^2 (4.4 ksi) using the relation $N_{u,30} = N_{u,test} \times (30/f_{cc,150,test})^{0.5}$. It is notable that the mean ultimate load capacity after crack cycling with a constant bearing pressure of $2.5 \times f_{cc,150}$ is slightly larger than that for monotonic loading or that after crack cycling with bearing pressure $1.0 \times f_{cc,150}$. This is again attributed to compaction of the concrete around the head of the anchor during crack cycling without significant reduction of the effective depth.

Influence of crack closure

Applying compression force to the anchorage component during crack cycling negatively affects anchor performance. This is largely due to crushing of the concrete around the anchor's load transfer point, for example, the anchor head. It may be assumed that compression loads applied to the anchorage component beyond those required to achieve crack closure around the loaded anchor would not continue to affect anchor load-displacement behavior because the compression loads would be transferred through the surrounding anchorage material (Fig. 21).

This hypothesis was investigated using headed studs located in anchorage components subjected to crack cycling with three different compression load levels ($F_2 = -50$ kN [11 kip],

$F_2 = 350$ kN [79 kip], and $F_2 = -500$ kN [112 kip]). These load levels correspond to stresses in the anchorage component of approximately 2, 10, and 15% of concrete compressive strength $f_{cc,150}$. The compressive load $F_2 = 50$ kN (11 kip) closed the crack only to approximately $\Delta w = 0.1$ mm (0.004 in.) during the initial crack cycle. Both of the load levels $F_2 = -350$ kN (79 kip) and $F_2 = -500$ kN (112 kip) were sufficient for full crack closure during the initial crack cycle.

Figure 22 shows the anchor displacement as a function of the number of crack cycles relative to the displacement in the

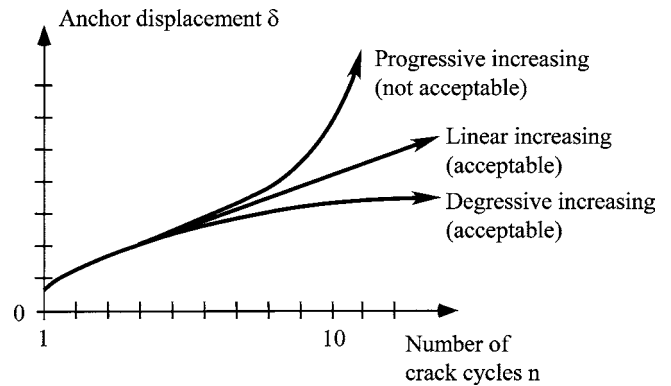


Fig. 18—Schematic anchor displacement for small number of crack cycles (<100) of relatively large amplitude, $w_1 - w_2 \geq 0.5$ mm (0.02 in.).

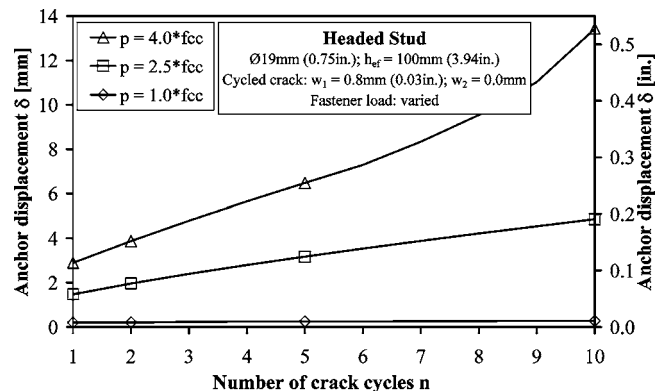


Fig. 19—Anchor displacement as function of number of crack cycles for varying head bearing pressure.

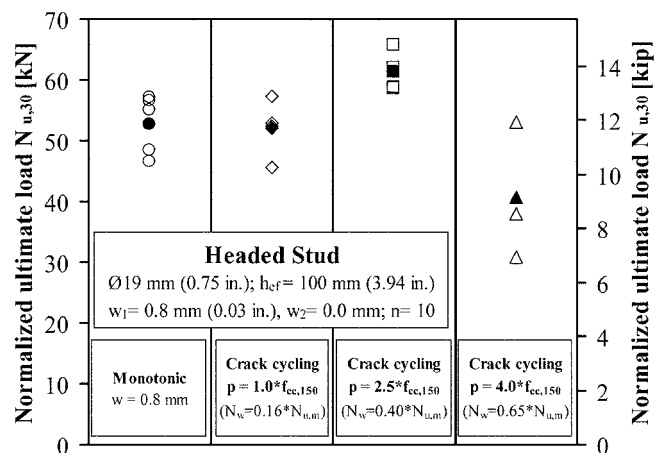


Fig. 20—Residual load for headed studs in large cycled cracks with varying head bearing pressure (solid symbol = mean).

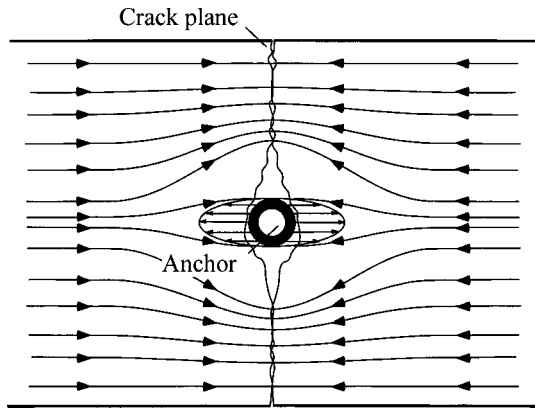


Fig. 21—Compressive load transfer around anchor (plan view).

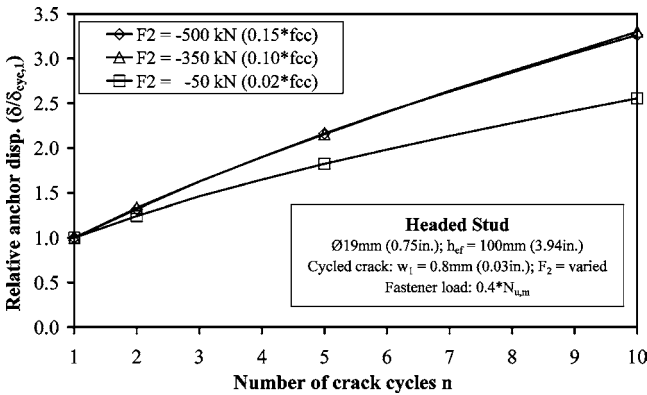


Fig. 22—Relative anchor displacement as function of number of crack cycles for varying anchorage component compression load.

first cycle for the various compressive load levels on the anchorage component. Each curve represents the average of three or more test replicates.

The results in Fig. 22 support the hypothesis that compression loads beyond those required to achieve full crack closure do not further affect the anchor displacement behavior during crack cycling. This can be seen in that the rate of anchor displacement increased between the cases with $F_2 = 50$ kN (11 kip) and $F_2 = -350$ kN (79 kip), that is, as the crack went from almost closed to fully closed, but stopped increasing for compression load greater than $F_2 = -350$ kN (79 kip). For all three cases, the residual strengths obtained in pullout tests performed subsequent to the crack cycling were close to those obtained in comparable monotonic reference tests.

Based on the test results, a compressive stress of $0.15 \times f_{cc,150}$ applied over the gross cross section area of the anchorage component appears to be sufficient to achieve full crack closure for anchor testing. Further research is needed, however, to verify this value.

CONCLUSIONS

The following conclusions can be drawn from the research results:

- Anchors may be subjected to crack cycling during an earthquake. Ten cycles ($n_{eq} = 10$) of crack opening to $w_1 = 0.8$ mm (0.03 in.) and crack closing to $w_2 = 0.0$ mm are considered to represent a worst-case scenario for anchors installed outside of plastic hinges in beam and column members;

- The behavior of anchors under simulated seismic crack cycling varies depending on the anchor failure mode and can be categorized based on the amount of displacement during crack cycling relative to the displacement at ultimate load in a corresponding static pullout test in an open crack;
- Anchors failing by concrete cone breakout can undergo displacements during crack cycling greater than those recorded at ultimate load in corresponding reference tests without significant reduction of the residual strength;
- The load-displacement curve for mechanical anchors failing by pull-through in crack cycling tests is bounded by the monotonic envelope from corresponding reference tests;
- Based on the available evidence, screw anchor displacement during crack cycling is limited to a fraction of the anchor thread spacing;
- A linear or degressive increase in anchor displacement as a function of the number of crack cycles (linear-linear scale) is one indicator of suitable anchor performance. The acceptable anchor displacement, however, is also influenced by other considerations, for example, the behavior of grouped anchors. Research is needed to evaluate the acceptable value of displacement during seismic crack cycling;
- The loaded anchor bearing pressure of $8f_c$ ($6.4f_{cc,150}$) used for nonseismic applications appears to be a suitable limit for representative seismic crack cycling;
- Compressive load on the anchorage component significantly increases anchor displacement during crack cycling. The influence of the compressive load disappears after the crack in the component has closed sufficiently around the anchor; and
- The behavior of anchors is significantly influenced by crack cycling of the type discussed in this paper. Crack cycling tests that simulate seismic conditions should be incorporated in ACI 355.2-04⁷ for anchors intended to resist seismic loads. A necessary precursor to the development of such tests is to establish acceptable displacement limits for these applications. Suitable displacement limits will likely be application dependent.

NOTATION

A_h	=	anchor head bearing area
a	=	anchor undercut length
d or \emptyset	=	shaft diameter of headed stud or thread diameter of screw anchor
d_0	=	drill hole diameter
d_h	=	diameter of anchor head
F_2	=	prescribed member compression load
f_c	=	concrete cylinder (Ø150 x 300 mm [Ø6 x 12 in.]) compressive strength
$f_{cc,150}$	=	concrete cube (150 mm [6 in.]) compressive strength
$F_{m,1}$	=	member load required to achieve w_1
$F_{m,2}$	=	member load required to achieve w_2 or F_2
h_{ef}	=	effective embedment depth of anchor
N	=	axial anchor load
N_w	=	sustained axial load on anchor
n	=	number of crack cycles
n_{eq}	=	number of equivalent crack cycles
p	=	anchor head bearing pressure
s_{cr}	=	crack spacing
w	=	crack width
w_1	=	prescribed crack opening width
w_2	=	prescribed crack closing width
$\Delta\delta$	=	change of anchor displacement
Δw	=	crack opening
δ	=	anchor displacement

REFERENCES

1. Sippel, T. M.; Asmus, J.; and Eligehausen, R., "Safety Concepts for Fastenings in Nuclear Power Plants," *Connections between Steel and Concrete*, RILEM Proceedings PRO 21, V. 1, 2001, pp. 564-575.
2. Rehm, G., and Lehmann, R., "Untersuchungen mit Metallspreizdübeln in der Gerissenen Zugzone von Stahlbetonbauteilen (Investigations with Metal Expansion Anchors in Cracked Reinforced Concrete Members)," FMFA, Universität Stuttgart, Germany, 1982, 392 pp. (in German)
3. Furche, J., "Versuchseinrichtung zur Prüfung von in Rissen verankerten Dübeln und erste Versuche an Parallelrisskörpern (Test Setup for the Testing of Fasteners in Cracks and Initial Tests in Parallel Cracks)," Institut für Werkstoffe im Bauwesen, Universität Stuttgart, Germany, 1987, 81 pp. (in German)
4. Furche, J., "Versuche an Kopfbolzen mit unterschiedlichen Kopf- formen bei Verankerungen in sich öffnenden und schließenden Rissen, (Tests with Headed Bolts with Various Head Shapes in Opening and Closing Cracks)," Report No. 9/5-88/10, Institut für Werkstoffe im Bauwesen, Universität Stuttgart, 1988, 194 pp. (in German)
5. Furche, J., "Einfluß der Hinterschnittform auf das Last-Verschiebungsverhalten bei zentrischem Zug: Teil III: Verschiebungsverhalten von Verankerungen in sich öffnenden und schließenden Rissen (Influence of the Undercut Shape on the Load-Displacement Behavior under Centric Tension Load: Part III: Displacement Behavior in Opening and Closing Cracks)," Report No. 9/8-90/8, Institut für Werkstoffe im Bauwesen, Universität Stuttgart, 1990, 84 pp. (in German)
6. Lotze, D., and Faoro, M., "Rißbreitenentwicklung und Dübelverschiebung bei veränderliche Bauteilbelastung (Crack Width Development and Fastener Displacement under Varying Building Component Loads)," Report No. 1/28-88/3, Institut für Werkstoffe im Bauwesen, Universität Stuttgart, 1988, 41 pp. (in German)
7. ACI Committee 355, "Qualification of Post-Installed Mechanical Anchors in Concrete (ACI 355.2-04) and Commentary (355.2R-04)," American Concrete Institute, Farmington Hills, MI, 2004, 31 pp.
8. ACI Committee 318, "Building Code Requirements for Structural Concrete (ACI 318-05) and Commentary (318R-05)," Farmington Hills, MI, 2005, 430 pp.
9. European Committee for Standardization (CEN), EN 1992-1-1, "Design of Concrete Structures: Part 1 General Rules and Rules for Buildings," Eurocode 2, 2004, 225 pp.
10. Hoehler, M. S., "Behavior and Testing of Fastenings to Concrete for Use in Seismic Applications, PhD dissertation, Universität Stuttgart, Stuttgart, Germany, 2006, 261 pp.
11. Krawinkler, H.; Zohrei, M.; Lashkari-Irvani, B.; Cofie, N. G.; and Hadidi-Tamjed, H., "Recommendation for Experimental Studies on the Seismic Behavior of Steel Components and Materials," Report No. NSF/CEE-83220, Stanford University, 1983, 251 pp.
12. Malhotra, P. K., "Cyclic-Demand Spectrum," *Earthquake Engineering and Structural Dynamics*, V. 31, No. 7, 2002, pp. 1441-1457.
13. Dutta, A., and Mander, J. B., "Energy Based Methodology for Ductile Design of Concrete Columns," *Journal of Structural Engineering*, V. 127, No. 12, 2002, pp. 1374-1381.
14. Kunnath, S. K., and Chai, Y. H., "Cumulative Damage-Based Inelastic Cyclic Demand Spectrum," *Earthquake Engineering and Structural Dynamics*, V. 33, No. 4, 2004, pp. 499-520.
15. Eligehausen, R.; Mallée, R.; and Silva, J. F., *Anchorage in Concrete Construction*, Ernst & Sohn, Berlin, Germany, 2006, 391 pp.
16. Eligehausen, R.; Mattis, L.; Wollmershauser, R.; and Hoehler, M. S., "Testing Anchors in Cracked Concrete—Guidance for Testing Laboratories: How to Generate Cracks," *Concrete International*, V. 26, No. 7, July 2004, pp. 66-71.
17. Deutsches Institut für Normung (DIN), "Tragwerke aus Beton, Stahlbeton und Spannbeton: Teil 2 Festlegung, Eigenschaften, Herstellung und Konformität (Concrete, Reinforced Concrete and Prestressed Concrete Structures: Part 2, Regulation, Properties, Production and Conformity)," DIN 1045, Berlin, Germany, 2001, 48 pp. (in German)
18. Deutsches Institut für Normung (DIN), "Prüfverfahren für Beton (Test Methods for Concrete)," DIN 1048, Berlin, Germany, 1991, 148 pp. (in German)
19. Furche, J., "Zum Trag- und Verschiebungsverhalten von Kopfbolzen bei zentrischem Zug (Load-Bearing and Displacement Behavior of Headed Bolts under Centric Tension Load)," PhD dissertation, Universität Stuttgart, Germany, 1994, 191 pp. (in German)